Check for updates

How to cite: *Angew. Chem. Int. Ed.* **2021**, *60*, 7174–7179
International Edition: doi.org/10.1002/anie.202014813
German Edition: doi.org/10.1002/ange.202014813

Helical Polymers

Helicity- and Molecular-Weight-Driven Self-Sorting and Assembly of Helical Polymers towards Two-Dimensional Smectic Architectures and Selectively Adhesive Gels

Yan-Xiang Li[+]*, Lei Xu*[+]*, Shu-Ming Kang, Li Zhou, Na Liu, and Zong-Quan Wu**

Abstract: *Self-sorting plays a crucial role in living systems such as the selective assembly of DNA and specific folding of proteins. However, the self-sorting of artificial helical polymers such as biomacromolecules has rarely been achieved. In this work, single-handed helical poly(phenyl isocyanide)s bearing pyrene (Py) and naphthalene (Np) probes were prepared, which exhibited interesting self-sorting properties driven by both helicity and molecular weight (M_n) in solution, solid state, gel, and on the gel surface as well. The polymers with the same helix sense and similar M_n can self-sort and assemble into well-defined two-dimensional smectic architectures and form stable gels in organic solvents. In contrast, mixed polymers with opposite handedness or different M_n were repulsive to each other and did not aggregate. Moreover, the gels of helical polymers with the same handedness and similar M_n can recognize themselves and adhere together to form a gel.*

Introduction

Helical structures adopted by biological macromolecules have played indispensable effects in living system such as the double helix of deoxyribonucleic acid (DNA) and α-helix of peptides and proteins.[1–3] The fundamental biological processes such as recognition, catalysis, replication, and heredity are related to helix structures.[4,5] Self-sorting is one of the fidelity recognition processes, in which a complex object can recognize self from non-self and further self-assembly into well-defined supramolecular architectures.[6–11] Biomacromolecules have powerful self-sorting ability, for example proteins and enzymes can discriminate two enantiomers through supramolecular interactions and thus facilitate biological processes.[12–15] These chirality-driven self-sorting processes are also depending on the handedness of the helical structures. Although a variety of synthetic self-sorting complexes, driven by metal-ligand coordination, hydrogen bonding, solvophobic interaction, etc.,[16–24] have been intensely investigated, bioinspired chirality-driven self-sorting systems have been rarely investigated and were mainly limited to discrete organic/coordination assemblies.[25–27] However, self-sorting of enantiomeric molecules is an effective strategy to achieve optically active materials via stereoselective self-assembly. The chiral auto-resolution in which the molecular components sort themselves into enantiomeric pure assemblies is analogous to Louis Pasteur's resolution on racemic sodium tartrate to form conglomerate crystals.[13,28,29]

To the best of our knowledge, helicity-driven self-recognition in synthetic assemblies like those in DNA and proteins is seldom reported. Possible reasons are that single-handed helical polymers without any chiral moieties, in which the chirality solely comes from the helix-sense, are very rare.[30–33] Moreover, the reported helical polymers usually have no specific recognition units or the units are far from the chiral moieties. The strong intermolecular interactions and chain entanglement between long polymer chains usually lead to stereocomplexes of chiral polymers.[34] However, helicity-driven self-sorting is particularly intriguing because it may be closely related to the origin of homochirality in Nature, and also attractive to the research fields of chirality recognition, enantiomer separation, chiral self-assembly and so on.[30,35]

Among the developed helical polymers, polyisocyanide is of great interesting, because of its unique rod-like helical structure and wide applications.[36–42] Polyisocyanide is generally prepared via the polymerization of the corresponding isocyanide monomer by using transition metal complexes or cations as catalysts.[43–46] However, the recent emerging mononuclear alkyne-palladium(II) catalysts is of particular useful, which can catalyze living polymerizations of various isocyanides and efficiently produce stereoregular polyisocyanides in high yields with expected molecular weight (M_n) and low polydispersity (M_w/M_n).[32,47,48] Taking advantage of this method, a variety of polyisocyanides in different topologies and broad applications have been facilely prepared.[49–54] One of the remarkable attributes of polyisocyanide in practical applications is its inherent chirality of the helical backbone because left- and right-handed helices are the mirror image of one another. Thus, investigating the interaction and recognition of helical polymer itself and disclose the influence of helicity and M_n on the recognition and self-sorting are of great interesting, which may pave a new avenue toward stereoselective fabrication of chiral architectures.

Recently, we have realized a controlled synthesis of single-handed helical polyisocyanide from achiral isocyanide monomer using the alkyne-Pd^{II} catalyst carrying chiral phosphine ligands.[32,48] The large optical activity of the

---

[*] Y.-X. Li,[+] L. Xu,[+] S.-M. Kang, Dr. L. Zhou, Dr. N. Liu,
Prof. Dr. Z.-Q. Wu
Department of Polymer Science and Engineering
School of Chemistry and Chemical Engineering
and Anhui Key Laboratory of Advanced Catalytic Materials and
Reaction Engineering, Hefei University of Technology
Hefei 230009, Anhui Province (China)
E-mail: zqwu@hfut.edu.cn

[+] These authors contributed equally to this work.

Supporting information and the ORCID identification number(s) for the author(s) of this article can be found under: https://doi.org/10.1002/anie.202014813.

© 2021 Wiley-VCH GmbH

resulting polyisocyanides was solely from the single-handed helicity, and inexistence of any other chiral moieties on the chain ends nor on the pendants. This kind of polymers are ideal systems to investigate the helicity- and M_n-driven self-sorting and assembly processes. In this work, we designed and synthesized a family of single-handed helical polyisocyanides with controlled M_n and low polydispersity bearing pyrene (Py) and naphthalene (Np) probes on the pendants. Fluorescence resonance energy transfer (FRET) and atomic force microscope (AFM) studies revealed these polymers can recognize themselves and self-sort in solution, solid state, in gel and on gel surface, through the discrimination on their helicity and M_n. Polyisocyanides with the same handedness can recognize themselves and self-assemble into well-defined two-dimensional (2D) smectic architectures. While the polymers with opposite handedness or largely different in M_n are repulsive to each other and couldn't aggregate together. Moreover, owing to strong intermolecular attraction, helical polymers with the same helicity can form a self-standing gel in various solvents. The gels could also recognize themselves, and selectively adhere together and self-healing based on the discrimination on helicity and M_n. The distinct 2D-smectic architectures with interesting self-recognition and self-healing properties endow the helical polymers with great potentials in many fields such as liquid crystallization, self-healing smart materials, stereoselective aggregation, photonic crystals, and in circularly polarized luminescence.[55,56]

Results and Discussion

Synthesis of single-handed helical polymers. As displayed in Scheme 1, single-handed helical polyisocyanides bearing Py or Np probes on the pendants were prepared via the helix-sense-specific living copolymerization of achiral isocyanide monomer (**1**) with **1**-Py or **1**-Np, respectively bearing Py- or Np-substituent (ca. 10% content), using Pd^{II} catalysts carrying *S*- or *R*-2,2′-bis(diphenylphosphino)-1,1′-binaphthalene (*S*- or *R*-BINAP) ligands.[32] Because of the living and helix-sense specific characters of the polymerization, a series of left-handed helices (*M*-poly-**1m**-Py, *M*-poly-**1m**-Np) and right-handed polymers (*P*-poly-**1m**-Py, and *P*-poly-**1m**-Np) containing Py- and Np-probes were facilely prepared with controlled molecular weights ($M_n = 19.6$–76.2 kDa) and low polydispersity ($M_w/M_n = 1.20$–1.26) (Table S1, Supporting Information (SI)). For comparison, left-handed *M*-poly-**1ms** and right-handed *P*-poly-**1ms** without fluorescent labelling were also prepared. The chemical structures of these polymers were fully characterized by size exclusion chromatography (SEC), ^{1}H NMR, and FT-IR as well (Figure S1–S13, SI).

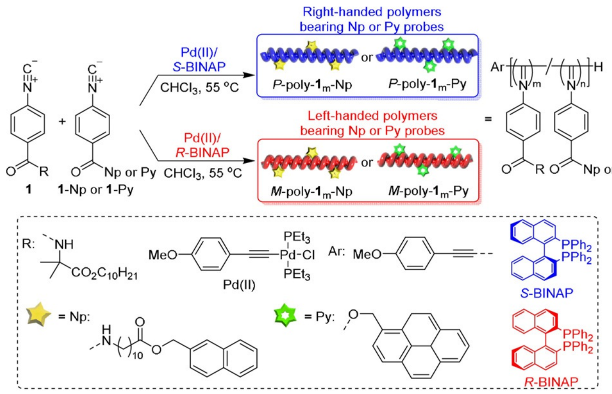

Scheme 1. Synthesis of the single-handed helical polymers bearing Np- or Py-probes.

The helix-sense of the synthetic polymers was verified by absorption and circular dichroism (CD) spectroscopies, and AFM analyses. As expected, left-handed *M*-poly-$\mathbf{1}_{150}$-Py and *M*-poly-$\mathbf{1}_{150}$-Np showed intense negative CD at the first Cotton band. While right-handed *P*-poly-**1m**-Np and *P*-poly-**1m**-Py showed positive CDs at the same absorption area, and were mirror image to that of *M*-poly-**1m**-Py and *M*-poly-**1m**-Np, regardless of the fluorescence probes (Figure S14, SI). The absolute molar CD intensities at 364 nm ($\Delta\varepsilon_{364}$) that quantitative reflect the enantiomeric excess of one-handed helix (ee_h) were up to 20 $M^{-1}cm^{-1}$ for all the polymers. Thus, the ee_h values of these polymers were higher than 99%, confirmed the single-handed helix-sense of the main chain.[32,48] Additional evidence for the single-handed helical structure came from the direct AFM observations. Only left-handed polymer chains could be observed on the AFM image of *M*-poly-**1m**-Py, while AFM images of *P*-poly-**1m**-Py polymers only showed right-handed helical chains (Figure S15, SI). The ee_h values of the polymers estimated by AFM were generally agree with the CD analyses, and were all up to 99%.[32,48] These studies convinced the single-handed helicity of the synthetic polyisocyanides bearing Py- and Np-probes. Note that all these polymers have the same chemical structure except for the helicity and fluorescent probes. The chiral ligand and the Pd^{II}-terminus were removed after the polymerization.[32] The helical structures were quite stable, no racemization was observed in THF at 55 °C for one week, probably due to the stabilization by the long alkyl tails and amide functions (Figure S16, SI).[48]

Helicity-driven self-sorting. Self-sorting capability of the helical polyisocyanides was first investigated in THF by FRET method.[23] Py-Labelled, right-handed *P*-poly-$\mathbf{1}_{150}$-Py and left-handed *M*-poly-$\mathbf{1}_{150}$-Py were, respectively added to two THF solutions of Np-labeled right-handed *P*-poly-$\mathbf{1}_{150}$-Np under the same condition (Figure 1a). The M_n of the three polymers were almost the same (Table S1, SI). Fluorescence spectra of the two mixtures were excited at 290 nm and the emission intensities at 435 nm of Py and 336 nm of Np were monitored. Figure 1b showed the time-dependent fluorescence spectra of the mixture of *P*-poly-$\mathbf{1}_{150}$-Py with *P*-poly-$\mathbf{1}_{150}$-Np. It was found that the Np-emission at 310–390 nm was gradually decreased, accompanied by a dramatically enhanced Py-emission at 390–550 nm. After ca. 144 h, the fluorescence spectra reached to a maximum and became constant. The remarkable FRET indicated the dynamic chain exchange and aggregation of the two polymers. In sharp contrast, almost no FRET could be detected on the mixture of *P*-poly-$\mathbf{1}_{150}$-Np and *M*-poly-$\mathbf{1}_{150}$-Py under the same conditions, even it was incubated for more than one week (Figure 1c). The structure of *P*-poly-$\mathbf{1}_{150}$-Py and *M*-poly-$\mathbf{1}_{150}$-Py was similar except for the helicity, thus the different FRET behaviors of

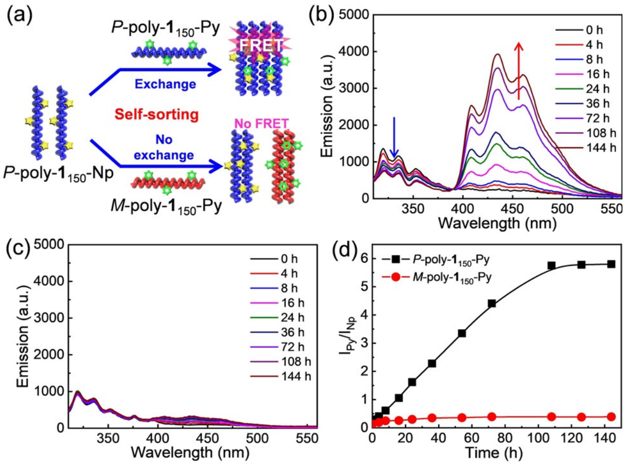

Figure 1. a) Schematic illustration of helicity-triggered self-sorting of single-handed helical polymers. Time-dependent fluorescence spectra of *P*-poly-**1**$_{150}$-Np in THF upon the addition of equivalent *P*-poly-**1**$_{150}$-Py (b) and *M*-poly-**1**$_{150}$-Py (c) at 25 °C. d) Plot of I_{Py}/I_{Np} values of *P*-poly-**1**$_{150}$-Np with the presence of *P*-poly-**1**$_{150}$-Py (black line), and *M*-poly-**1**$_{150}$-Py (red line) versus incubation time.

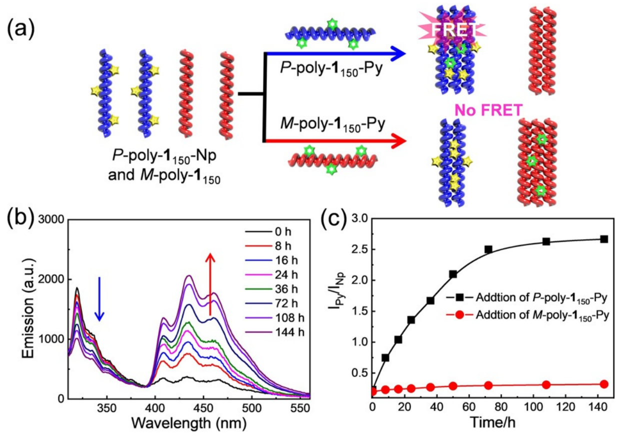

Figure 2. a) Schematic illustration for the helicity-triggered selective chain exchange and aggregation. b) Time-dependent fluorescent spectra of equivalent mixtures of *P*-poly-**1**$_{150}$-Np/*M*-poly-**1**$_{150}$ in THF with the presence of *P*-poly-**1**$_{150}$-Py at 25 °C ($c = 0.05$ mg mL^{-1}). c) Plot of I_{Py}/I_{Np} values against the incubation time of the *P*-poly-**1**$_{150}$-Np/*M*-poly-**1**$_{150}$ mixture with the presence of *P*-poly-**1**$_{150}$-Py (black line) and *M*-poly-**1**$_{150}$-Py (red line), respectively.

the two mixtures can be ascribed to the incompatibility of the opposite helicity. That is the helical polymers with the same handedness can dynamic exchanged and aggregated together, while the mixed polymers with opposite handedness were repulsive to each other and self-sorted. The helicity-driven self-sorting was further investigated by treating two THF solutions of *P*-poly-**1**$_{150}$-Np, respectively with various amounts of *M*-poly-**1**$_{150}$-Py and *P*-poly-**1**$_{150}$-Py under identical conditions. The addition of *P*-poly-**1**$_{150}$-Py induced a clear FRET due to the chain exchange and aggregation of the two polymers with the same helicity, even only 0.1 equivalent of *P*-poly-**1**$_{150}$-Py was added (Figure S17a, SI). In contrast, no FRET could be discerned upon the addition of *M*-poly-**1**$_{150}$-Py with the opposite handedness to that of *P*-poly-**1**$_{150}$-Np, even 20 times equivalent were used (Figure S17b,SI). These results confirmed that the helicity can drive the polymers to recognize themselves and self-sorted in solution.

The primary results suggested the helical polymer can recognize self from non-self in mixed complexes with similar structures. To further verify this self-recognition process, two equivalent mixtures of *P*-poly-**1**$_{150}$-Np and unlabeled *M*-poly-**1**$_{150}$ solutions were, respectively treated with *P*-poly-**1**$_{150}$-Py and *M*-poly-**1**$_{150}$-Py under identical conditions (Figure 2 a). As anticipated, the addition of *P*-poly-**1**$_{150}$-Py gradually induced an intense Py-emission at 390–550 nm through FRET process (Figure 2 b), and the emission increased with the incubation time. Whereas, the addition of *M*-poly-**1**$_{150}$-Py to the *P*-poly-**1**$_{150}$-Np/*M*-poly-**1**$_{150}$ mixture could not induce detectable FRET (Figure S18, SI). Accordingly, similar dynamic polymer exchange was also observed on the respective additions of *M*-poly-**1**$_{150}$-Py and *P*-poly-**1**$_{150}$-Py to the mixtures containing equivalent amount of unlabeled *P*-poly-**1**$_{150}$ and Np-labelled *M*-poly-**1**$_{150}$-Np. In which only *M*-poly-**1**$_{150}$-Py could induced FRET of the mixture. These results crucially suggested that the dynamic polymer chain exchange and aggregation exclusively occurred among the polymers with the same helicity, and further supported the helical polymers can recognize themselves via the discrimination on helix-sense.

The abovementioned helicity-driven self-sorting of helical polymers could occur in other common solvents, including $CHCl_3$, toluene, *n*-hexane, and *n*-dodecane (Figure S19, SI). While THF is the best among the tested solvents. The self-sorting behavior was related the solvation ability of the solvents (Table S2), the higher solvation ability, the better self-sorting. Moreover, temperature also paly important role on the recognition and self-sorting process. As shown in Figure S20 in SI, the helicity-driven dynamic polymer chains exchange was faster at evaluated temperature. Quantitative analysis on the self-sorting kinetics revealed that it was about 6.5 times faster at 25 °C than that at 5 °C (Figure S20f, SI). Because the higher temperature can accelerate the thermal motion of polymer chains and then facilitate the disassembly and self-assembly process.

Remarkably, helicity-driven self-sorting had clearly be observed on the equivalent mixtures of *M*-poly-**1**$_{200}$-Py/*M*-poly-**1**$_{200}$-Np, *M*-poly-**1**$_{150}$-Py/*M*-poly-**1**$_{150}$-Np, *M*-poly-**1**$_{100}$-Py/*M*-poly-**1**$_{100}$-Np, and *M*-poly-**1**$_{50}$-Py/*M*-poly-**1**$_{50}$-Np in same helicity and similar M_n values (Figure S21, SI). While the rate and extent of the self-sorting were different and depending on M_n of the mixtures. The mixed polymers with higher M_n values can induced intense FRET more quickly (Figure S21d, SI), indicating the longer polymer chains, the stronger intermolecular interactions. For example, the mixture of *M*-poly-**1**$_{200}$-Py/*M*-poly-**1**$_{200}$-Np reached a balance FRET within 72 h, while it took ca. 168 h to get a balance for the mixture of *M*-poly-**1**$_{50}$-Py/*M*-poly-**1**$_{50}$-Np with shorter chain length (Figure S21, SI). These results suggested the higher M_n can promote the helicity-driven recognition and self-sorting.

The effect of M_n on the helicity-driven self-sorting inspired us to investigate whether chain-length can promote the self-sorting process alone (Figure 3 a). Thus, five Py-

© 2021 Wiley-VCH GmbH

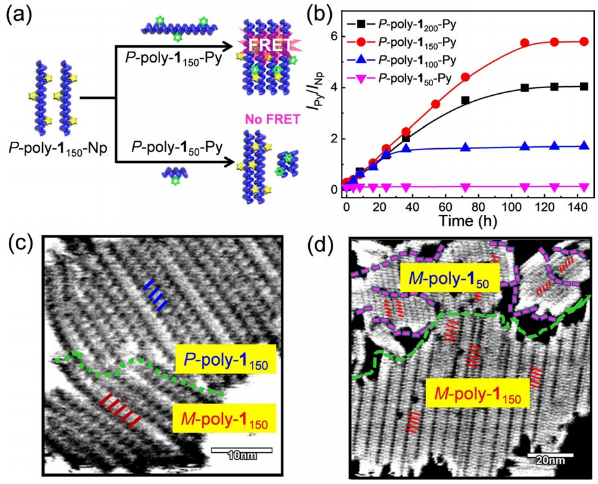

Figure 3. a) Schematic illustration of chain length triggered polymer chain exchange and aggregation. b) Plot of I_{Py}/I_{Np} versus incubation time of P-poly-$\mathbf{1}_{150}$-Np with the presence of P-poly-$\mathbf{1}_{200}$-Py (black line), P-poly-$\mathbf{1}_{150}$-Py (red line), P-poly-$\mathbf{1}_{100}$-Py (blue line), and P-poly-$\mathbf{1}_{50}$-Py (pink line) in THF at room temperature. AFM images of M-poly-$\mathbf{1}_{150}$/P-poly-$\mathbf{1}_{150}$ (c), and M-poly-$\mathbf{1}_{150}$/M-poly-$\mathbf{1}_{50}$ (d) mixtures cast from THF solution on HOPG at 25 °C.

labelled right-handed polymers (P-poly-$\mathbf{1}_{50}$-Py, P-poly-$\mathbf{1}_{80}$-Py, P-poly-$\mathbf{1}_{100}$-Py, P-poly-$\mathbf{1}_{150}$-Py, and P-poly-$\mathbf{1}_{200}$-Py) with different M_n values and low dispersity ($M_w/M_n = 1.21$–1.26) were, respectively added to five THF solutions of P-poly-$\mathbf{1}_{150}$-Np at 25 °C under the same condition. Although all the polymers were right-handed, the process of the self-sorting and the dynamic polymer chain exchange were quite different and were related to M_n (Figure 3b, and Figure S22 in SI). The mixed polymers with similar M_n (P-poly-$\mathbf{1}_{150}$-Py/P-poly-$\mathbf{1}_{150}$-Np) can quickly induced a strong FRET, while the mixed P-poly-$\mathbf{1}_{150}$-Np/P-poly-$\mathbf{1}_{50}$-Py with large different M_n couldn't induced a remarkable FRET under the same condition. These results suggested the difference in M_n played important effect on the self-sorting process. Accordingly, the mixtures of left-handed helices with different M_n values also exhibited similar FRET results, which confirmed the helical polymers can recognize themselves via the differentiation on both helicity and M_n. It is worthy to mention that all the tested polymers with different M_n values have good solubility in THF, and the self-sorting experiments were carried out at the concentration much lower than their solubility (Table S3).

Self-assembled 2D-smectic architectures. The morphology of the self-sorted helical polymers was then investigated. AFM studies revealed the helical polymers were self-assembled into well-defined 2D-smectic structures. Figure 3c displayed the AFM image casted from THF solution of the equivalent mixture of M-poly-$\mathbf{1}_{150}$/P-poly-$\mathbf{1}_{150}$ on highly oriented pyrolytic graphite (HOPG).[32,41,48] The helical polymer chains were parallel bundled together into a single molecular layer film with ca. 2.20 nm in height (Figure S23, SI). The average length of polymer chains was ca. 38 nm and in good homogeneity. It was found that the polymers were self-sorted based on the helix-sense, and the same handed helices were closely bundled together into 2D-smectic structures through differentiation on the helicity. The boundary of the right- and left-handed helical polymer domains can be clearly distinguished (green dotted line in Figure 3c). These results further confirmed the helicity-driven self-sorting of single-handed helical polymers can not only occurred in solution but also in solid state. Moreover, the M_n-driven self-sorting was also confirmed by AFM. AFM image of the equivalent mixture of M-poly-$\mathbf{1}_{150}$/M-poly-$\mathbf{1}_{50}$ casted from the THF solution was showed in Figure 3d. Two kind of polymers with chain length of ca. 38 and ca. 15 nm were clearly observed, which were, respectively corresponding to M-poly-$\mathbf{1}_{150}$ and M-poly-$\mathbf{1}_{50}$ polymers. As anticipated, the polymer chains were compacted bundle together into a single molecular layer film, and were compartmentalized into several 2D-smectic domains based on chain length (Figure 3d). In each domain, the polymers have similar chain lengths, further supported M_n-driven self-sorting of the helical polymers.

Self-sorting in gels. Because of strong intermolecular interactions, the helical polymers can form stable gels in organic solvents including n-hexane, n-dodecane and toluene. However, the gelation ability was also depending on the helicity and M_n. The mixed polymers with the same helicity and similar M_n were easily to form stable gels. For example, single-handed helices like M-poly-$\mathbf{1}_{150}$ (or P-poly-$\mathbf{1}_{150}$) can formed self-standing gels in n-hexane and n-dodecane with the concentration as low as 25 mg mL^{-1} (ca. 3 wt. %) (Figure 4a). In contrast, equivalent mixture of M-poly-$\mathbf{1}_{150}$ and P-poly-$\mathbf{1}_{150}$ with similar M_n but were opposite in handedness was hard to form a gel even the concentration was increased to 50 mg mL^{-1} and stand at room temperature for one week (Figure 4b). Rheology studies also supported the helicity-depending gelation, the storage moduli (G') of left-handed M-poly-$\mathbf{1}_{150}$ in n-dodecane was larger than the loss moduli (G'') for all the probed frequencies, indicative a typical gel-like material response (Figure 4e).[57] Similarly, right-handed P-poly-$\mathbf{1}_{150}$ showed a similar rheology behavior to that of M-poly-$\mathbf{1}_{150}$ due to the strong gelation ability. However, the rheology of the equivalent mixture of P-poly-$\mathbf{1}_{150}$/M-poly-$\mathbf{1}_{150}$ was quite different, the modulus values were several orders of

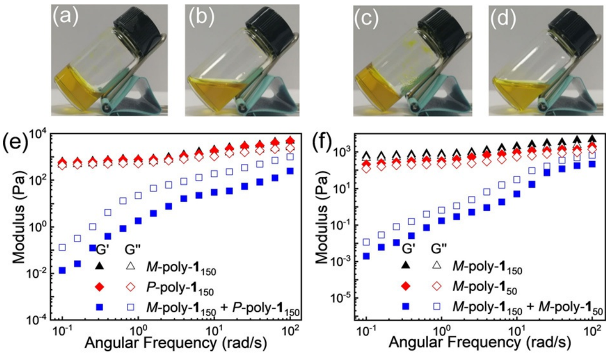

Figure 4. Photographs of M-poly-$\mathbf{1}_{150}$ (a), equivalent mixture of M-poly-$\mathbf{1}_{150}$/P-poly-$\mathbf{1}_{150}$ (b), M-poly-$\mathbf{1}_{50}$ (c), and equivalent mixture of M-poly-$\mathbf{1}_{150}$/M-poly-$\mathbf{1}_{50}$ (d) in n-dodecane at room temperature ($c = 25$ mg mL^{-1}). Viscoelastic moduli G' (ω) (closed symbols) and G'' (ω) (open symbols) for M-poly-$\mathbf{1}_{150}$ (black), P-poly-$\mathbf{1}_{150}$ (red) and equivalent mixture of M-poly-$\mathbf{1}_{150}$/P-poly-$\mathbf{1}_{150}$ (blue) (e), and M-poly-$\mathbf{1}_{150}$ (black), M-poly-$\mathbf{1}_{50}$ (red) and equivalent mixture of M-poly-$\mathbf{1}_{150}$/M-poly-$\mathbf{1}_{50}$ (blue) (f) recorded in n-dodecane.

magnitude smaller than those of pure *M*-poly-$\mathbf{1}_{150}$ or *P*-poly-$\mathbf{1}_{150}$. Moreover, the G' was dominant lower than G'', consistent to a typical solution-like rheology response.[57]

The single-handed helical polymers were prone to form a stable gel, even the degree of the polymerization (DP) was lower than 50. For instance, both *M*-poly-$\mathbf{1}_{150}$ and *M*-poly-$\mathbf{1}_{50}$ can independently formed self-standing gels in *n*-dodecane (Figure 4c). However, because of the M_n-driven self-sorting, the equivalent mixture of *M*-poly-$\mathbf{1}_{150}$/*M*-poly-$\mathbf{1}_{50}$ with the same helicity but different in M_n was hard to form a gel (Figure 4d), even the concentration was increased to 100 mg mL^{-1} and stand for one week. More evidences came from the rheology measurements. As outlined in Figure 4f, single handed helical polymers with low M_n also had high G' and G'' values. For example, the G' and G'' were 200 and 100 Pa for *M*-poly-$\mathbf{1}_{50}$, respectively, similar to those of *M*-poly-$\mathbf{1}_{150}$ with higher M_n. Remarkably, the mixture of long *M*-poly-$\mathbf{1}_{150}$ with short *M*-poly-$\mathbf{1}_{50}$ with the same left-handed helicity, the G' and G'' values decreased dramatically (Figure 4f). Furthermore, G' was clearly lower than G'', suggested the mixture of the two polymers was a solution-like state.[57] These results further confirmed the different intermolecular interaction between the polymers with different helicity and M_n, and also supported the self-sorting capability in gelation.

More interestingly, the helicity- and M_n-driven self-sorting of helical polymers also existed on gel surface, which endowed the gels with selective adhesion property. As depicted in Figure 5, the gels formed from helical polymers with the same helicity and similar M_n were very easy to adhere together due to the dynamic chain exchange on the interface of the two gels. For example, two cut *M*-poly-$\mathbf{1}_{150}$ gels can tightly adhere together and self-healed immediately when they were contacted together (Figure 5a, and video 1 in SI). Similar phenomenon was also observed on the cut *P*-poly-$\mathbf{1}_{150}$ gels (Figure 5b, and video 2 in SI). Tensile tests revealed the ultimate stress was ≈1.0 MPa for the original *P*-poly-$\mathbf{1}_{150}$ gel, and was 0.7 MPa for the repaired gel, indicated ca. 70% strength was recovered (Figure S24, SI). These results can be ascribed to the chain exchange between polymers with the same helicity on interface of the two gels. In sharp contrast, no adhesion and self-healing could be observed when the cut *M*-poly-$\mathbf{1}_{150}$ gel was contacted with *P*-poly-$\mathbf{1}_{150}$ gel (Figure 5c, and video 3 in SI), because of the helicity-driven self-sorting and slow chain exchange on the gel surface between the helical polymers with the opposite handedness. Similar results can also be found on the polymers with the same helicity but largely different in M_n. No adhesion was observed when the cut gels of long *M*-poly-$\mathbf{1}_{150}$ and short *M*-poly-$\mathbf{1}_{50}$ possessing the same helicity were contact together, even they were contacted together for 24 h (Figure S25, and video 4 and 5 in SI). These investigations revealed that the helical polymers can recognize themselves and selective adhered together and self-healing on the basis of both the helicity and M_n, not only in solution, in solid state, in gel, but also on gel surface.

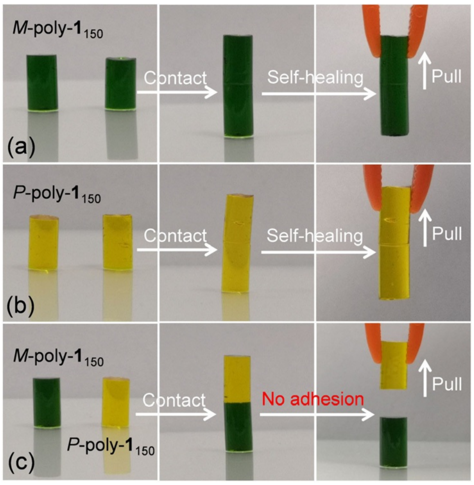

Figure 5. Photographs of selective adhesion and healing properties of *M*-poly-$\mathbf{1}_{150}$ gel (a), *P*-poly-$\mathbf{1}_{150}$ gel (b), and *M*-poly-$\mathbf{1}_{150}$ gel with *P*-poly-$\mathbf{1}_{150}$ gel (c). The gels were prepared in *n*-dodecane at room temperature. The *M*-poly-$\mathbf{1}_{150}$ gel was colored with methylene blue for comparison.

Conclusion

We have synthesized a series of Np- and Py-labelled, single-handed helical polyisocyanides. These polymers showed interestingly self-sorting properties driven by both the helicity and M_n. The helical polymers can recognize themselves through differentiation on either helicity or M_n in solution, solid state, gel and on gel surface as well, via dynamically chain exchange and aggregation processes. The present work not only achieve a breakthrough in self-recognition on complex macromolecular level, but also bring out an innovative stereoselective self-assembly strategy for fabricating dynamic supramolecular architectures applicable to various research fields such as self-recognition, chiral auto-resolution, liquid crystallization, self-healing materials and so on.

Acknowledgements

This work is supported by National Natural Science Foundation of China (NSFC, Nos. 21871073, 22071041, 51673057, 21971052, and 51903072). Z.W. and L.Z. thank the fundamental research funds for the central universities of China (Grant Nos. PA2019GDPK0057 and PA2020GDJQ0028).

Conflict of interest

The authors declare no conflict of interest.

Keywords: FRET · helical structures · recognition · self-assembly · self-sorting

---

[1] L. Pauling, R. B. Corey, H. R. Branson, *Proc. Natl. Acad. Sci. USA* **1951**, *37*, 205–211.
[2] J. D. Watson, F. H. C. Crick, *Nature* **1953**, *171*, 737–738.

© 2021 Wiley-VCH GmbH

[3] B. Alberts, A. Johnson, J. Lewis, D. Morgan, M. Raff, K. Roberts, P. Walter, *Molecular Biology of the Cell*, 6th ed., Garland Science, New York, **2014**.

[4] G. Wei, W. Xi, R. Nussinov, B. Ma, *Chem. Rev.* **2016**, *116*, 6516–6551.

[5] M. Madsen, K. V. Gothelf, *Chem. Rev.* **2019**, *119*, 6384–6458.

[6] M. Marguet, C. Bonduelle, S. Lecommandoux, *Chem. Soc. Rev.* **2013**, *42*, 512–529.

[7] C. F. J. Faul, *Acc. Chem. Res.* **2014**, *47*, 3428–3438.

[8] F. Hong, F. Zhang, Y. Liu, H. Yan, *Chem. Rev.* **2017**, *117*, 12584–12640.

[9] C. Dreaael, T. Reppe, M. Prehm, M. Brautzsch, C. Tschierske, *Nat. Chem.* **2014**, *6*, 971–977.

[10] Z. He, W. Jiang, C. A. Schalley, *Chem. Soc. Rev.* **2015**, *44*, 779–789.

[11] S. Onogi, H. Shigemitsu, T. Yoshii, T. Tanida, M. Ikeda, R. Kubota, I. Hamachi, *Nat. Chem.* **2016**, *8*, 743–752.

[12] S. Toda, L. R. Blauch, S. K. Y. Tang, L. Morsut, W. A. Lim, *Science* **2018**, *361*, 156–162.

[13] L. P. Garcǐa, D. B. Amabilino, *Chem. Soc. Rev.* **2007**, *36*, 941–967.

[14] C. Rest, M. J. Mayoral, G. Fernández, *Int. J. Mol. Sci.* **2013**, *14*, 1541–1565.

[15] A. M. Johnson, C. A. Wiley, M. C. Young, X. Zhang, Y. Lyon, R. R. Julian, R. J. Hooley, *Angew. Chem. Int. Ed.* **2015**, *54*, 5641–5645; *Angew. Chem.* **2015**, *127*, 5733–5737.

[16] C. Talotta, C. Gaeta, Z. Qi, C. A. Schalley, P. Neri, *Angew. Chem. Int. Ed.* **2013**, *52*, 7437–7441; *Angew. Chem.* **2013**, *125*, 7585–7589.

[17] A. Sarkar, S. Dhiman, A. Chalishazar, S. J. George, *Angew. Chem. Int. Ed.* **2017**, *56*, 13767–13771; *Angew. Chem.* **2017**, *129*, 13955–13959.

[18] S. Prasanthkumar, S. Ghosh, V. C. Nair, A. Saeki, S. Seki, A. Ajayaghosh, *Angew. Chem. Int. Ed.* **2015**, *54*, 946–950; *Angew. Chem.* **2015**, *127*, 960–964.

[19] J. van Herrikhuyzen, A. Syamakumari, A. P. H. J. Schenning, E. W. Meijer, *J. Am. Chem. Soc.* **2004**, *126*, 10021–10027.

[20] E. R. Draper, J. R. Lee, M. Wallace, F. Jckel, A. J. Cowanac, D. J. Adams, *Chem. Sci.* **2016**, *7*, 6499–6505.

[21] H. Frisch, E. Fritz, F. Stricker, L. Schmüser, D. Spitzer, T. Weidner, B. J. Ravoo, P. Besenius, *Angew. Chem. Int. Ed.* **2016**, *55*, 7242–7246; *Angew. Chem.* **2016**, *128*, 7358–7362.

[22] Y.-S. Wang, T. Feng, Y.-Y. Wang, F. E. Hahn, Y.-F. Han, *Angew. Chem. Int. Ed.* **2018**, *57*, 15767–15771; *Angew. Chem.* **2018**, *130*, 15993–15997.

[23] S. Imai, M. Takenaka, M. Sawamoto, T. Terashima, *J. Am. Chem. Soc.* **2019**, *141*, 511–519.

[24] R. Kramer, J. M. Lehn, A. Marquis-Rigault, *Proc. Natl. Acad. Sci. USA* **1993**, *90*, 5394–5398.

[25] L.-L. Yan, C.-H. Tan, G.-L. Zhang, L.-P. Zhou, J.-C. Bnzli, Q.-F. Sun, *J. Am. Chem. Soc.* **2015**, *137*, 8550–8555.

[26] L. J. Prins, J. Huskens, F. de Jong, P. Timmerman, D. N. Reinhoudt, *Nature* **1999**, *398*, 498–502.

[27] H. Jędrzejewska, M. Wierzbicki, P. Cmoch, K. Rissanen, A. Szumna, *Angew. Chem. Int. Ed.* **2014**, *53*, 13760–13764; *Angew. Chem.* **2014**, *126*, 13980–13984.

[28] Q. Xiao, J. D. Rubien, Z. Wang, E. H. Reed, D. A. Hammer, D. Sahoo, P. A. Heiney, S. S. Yadavalli, M. Goulian, S. E. Wilner, T. Baumgart, S. A. Vinogradov, M. L. Klein, V. Percec, *J. Am. Chem. Soc.* **2016**, *138*, 12655–12663.

[29] L. Pasteur, *Ann. Chim. Phys.* **1853**, *38*, 437–483.

[30] E. Yashima, K. Maeda, H. Iida, Y. Furusho, K. Nagai, *Chem. Rev.* **2009**, *109*, 6102–6211.

[31] Y. Dong, C. Yao, Y. Zhu, L. Yang, D. Luo, D. Yang, *Chem. Rev.* **2020**, *120*, 9420–9481.

[32] L. Xu, L. Yang, Z. Guo, N. Liu, Y.-Y. Zhu, Z. Li, Z.-Q. Wu, *Macromolecules* **2019**, *52*, 5698–5706.

[33] J.-H. Chu, X.-H. Xu, S.-M. Kang, N. Liu, Z.-Q. Wu, *J. Am. Chem. Soc.* **2018**, *140*, 17773–17781.

[34] J. C. Worch, H. Prydderch, S. Jimaja, P. Bexis, M. L. Becker, A. P. Dove, *Nat. Rev. Chem.* **2019**, *3*, 514–535.

[35] E. Yashima, N. Ousaka, D. Taura, K. Shimomura, T. Ikai, K. Maeda, *Chem. Rev.* **2016**, *116*, 13752–13990.

[36] Y. Wang, T. Harada, L. Q. Phuong, Y. Kanemitsu, T. Nakano, *Macromolecules* **2018**, *51*, 6865–6877.

[37] L. Xu, C. Wang, Y.-X. Li, X.-H. Xu, L. Zhou, N. Liu, Z.-Q. Wu, *Angew. Chem. Int. Ed.* **2020**, *59*, 16675–16682; *Angew. Chem.* **2020**, *132*, 16818–16825.

[38] S. Wang, X. Feng, J. Zhang, P. Yu, Z. Guo, Z. Li, X. Wan, *Macromolecules* **2017**, *50*, 3489–3499.

[39] J. J. L. M. Cornelissen, A. E. Rowan, R. J. M. Nolte, N. A. J. M. Sommerdijk, *Chem. Rev.* **2001**, *101*, 4039–4070.

[40] J. J. L. M. Cornelissen, M. Fischer, N. A. J. M. Sommerdijk, R. J. M. Nolte, *Science* **1998**, *280*, 1427–1430.

[41] E. Yashima, K. Maeda, Y. Furusho, *Acc. Chem. Res.* **2008**, *41*, 1166–1180.

[42] P. H. J. Kouwer, M. Koepf, V. A. A. Le Sage, M. Jaspers, A. M. van Buul, Z. H. Eksteen-Akeroyd, T. Woltinge, E. Schwartz, H. J. Kitto, R. Hoogenboom, S. J. Picken, R. J. M. Nolte, E. Mendes, A. E. Rowan, *Nature* **2013**, *493*, 651–655.

[43] K. Onitsuka, T. Mori, M. Yamamoto, F. Takei, S. Takahashi, *Macromolecules* **2006**, *39*, 7224–7231.

[44] G. A. Metselaar, J. J. L. M. Cornelissen, A. E. Rowan, R. J. M. Nolte, *Angew. Chem. Int. Ed.* **2005**, *44*, 1990–1993; *Angew. Chem.* **2005**, *117*, 2026–2029.

[45] Z.-Q. Wu, K. Nagai, M. Banno, K. Okoshi, K. Onitsuka, E. Yashima, *J. Am. Chem. Soc.* **2009**, *131*, 6708–6718.

[46] X. Yan, S. Zhang, P. Zhang, X. Wu, A. Liu, G. Guo, Y. Dong, X. Li, *Angew. Chem. Int. Ed.* **2018**, *57*, 8947–8952; *Angew. Chem.* **2018**, *130*, 9085–9090.

[47] Y.-X. Xue, Y.-Y. Zhu, L.-M. Gao, X.-Y. He, N. Liu, W.-Y. Zhang, J. Yin, Y. Ding, H. Zhou, Z.-Q. Wu, *J. Am. Chem. Soc.* **2014**, *136*, 4706–4713.

[48] L. Zhou, X.-H. Xu, Z.-Q. Jiang, L. Xu, B.-F. Chu, N. Liu, Z.-Q. Wu, *Angew. Chem. Int. Ed.* **2021**, *60*, 806–812; *Angew. Chem.* **2021**, *133*, 819–825.

[49] E. Elacqua, K. B. Manning, D. S. Lye, S. K. Pomarico, F. Morgia, M. Weck, *J. Am. Chem. Soc.* **2017**, *139*, 12240–12250.

[50] M. Su, N. Liu, Q. Wang, H. Wang, J. Yin, Z.-Q. Wu, *Macromolecules* **2016**, *49*, 110–119.

[51] E. Elacqua, A. Croom, K. B. Manning, S. K. Pomarico, D. Lye, L. Young, M. Weck, *Angew. Chem. Int. Ed.* **2016**, *55*, 15873–15878; *Angew. Chem.* **2016**, *128*, 16105–16110.

[52] L. Yang, Y. Tang, N. Liu, C.-H. Liu, Y. Ding, Z.-Q. Wu, *Macromolecules* **2016**, *49*, 7692–7702.

[53] Z.-Q. Jiang, S.-Q. Zhao, Y.-X. Su, N. Liu, Z.-Q. Wu, *Macromolecules* **2018**, *51*, 737–745.

[54] Q. Wang, B.-F. Chu, J.-H. Chu, N. Liu, Z.-Q. Wu, *ACS Macro Lett.* **2018**, *7*, 127–131.

[55] H. Jędrzejewska, A. Szumna, *Chem. Rev.* **2017**, *117*, 4863–4899.

[56] C. E. Diesendruck, N. R. Sottos, J. S. Moore, S. R. White, *Angew. Chem. Int. Ed.* **2015**, *54*, 10428–10447; *Angew. Chem.* **2015**, *127*, 10572–10593.

[57] J. P. Celli, B. S. Turner, N. H. Afdhal, R. H. Ewoldt, G. H. McKinley, R. Bansil, S. Erramilli, *Biomacromolecules* **2007**, *8*, 1580–1586.

Manuscript received: November 5, 2020
Revised manuscript received: January 6, 2021
Accepted manuscript online: January 7, 2021
Version of record online: February 24, 2021